Available online at www.eccomasproceedia.org
Eccomas Proceedia COMPDYN (2017) 2867-2878

ECCOMAS
Proceedia

COMPDYN 2017
6th ECCOMAS Thematic Conference on
Computational Methods in Structural Dynamics and Earthquake Engineering
M. Papadrakakis, M. Fragiadakis (eds.)
Rhodes Island, Greece, 15–17 June 2017

ROCKING RESONANCE CONDITIONS OF LARGE AND SLENDER RIGID BLOCKS UNDER THE INTENSE PHASE OF AN EARTHQUAKE

Claudia Casapulla[1], **Alessandra Maione**[2]

[1] University of Napoli "Federico II"
Department of Structures for Engineering and Architecture, Napoli, Italy
casacla@unina.it

[2] University of Napoli "Federico II"
Department of Structures for Engineering and Architecture, Napoli, Italy
arch.maione@gmail.com

Keywords: Multiple impulses, rigid block dynamics, rocking amplification, size effect, resonance effects.

Abstract. *A simplified approach is proposed in this paper for assessing the safety levels of the seismic response of large and slender rigid masonry blocks. The dynamic behavior of rigid free-standing blocks subjected to earthquake ground motions is highly non-linear and sensitive to small perturbations of various parameters. Many difficulties arise in defining reliable response spectra for such systems and these are well known in the literature. An artificial limit accelerogram is herein proposed to represent the most unfavorable effects of the intense phase of an earthquake. This consists of a sequence of instantaneous impulses, all applied right after the impact of the blocks on the ground. The resonance conditions also aim at highlighting to what extent the ground motion details and the system parameters can influence the rocking response. A secondary sequence of intermediate impulses is then introduced to reduce the resonance effects and to cover a broad range of conditions. Approximate equations of motion of the rocking blocks are also proposed and numerical analyses are performed to highlight the most significant aspects of the proposed approach.*

© 2017 The Authors. Published by Eccomas Proceedia.
Peer-review under responsibility of the organizing committee of COMPDYN 2017.
doi: 10.7712/120117.5612.17190

1 INTRODUCTION

Ancient masonry structures are generally regarded as sets of macro-elements under earthquake actions. The seismic vulnerability of these elements can be assessed throughout rocking analyses or energy-based approaches [1]. Rocking motion is frequently observed when the morphology of the wall sections allows a monolithic behavior. In this case, in absence of proper connections between orthogonal walls and between walls and floors, out-of-plane mechanisms may occur with discretization of the walls in few rigid macro-blocks articulated by hinges. Here rocking and sliding motions may take place. The analysis of the local failure modes is also provided by the multi-level approach of the Italian Guidelines on Cultural Heritage [2].

In order to evaluate the static load factor causing the onset of this kind of mechanisms, non-standard limit analysis procedures can be applied [3-9]. A dynamic approach, however, is useful to investigate the time-history evolution of the rocking response and the sensitivity to the features of the seismic action. Moreover, the response of a rocking block is extremely sensitive to boundary conditions, very relevant for masonry panels. In that sense, some methods were recently proposed to consider the interaction with transverse walls [10], roofs [11], or vertical restrainers [12].

From this perspective, the reference model for the rocking motion without sliding of a rigid block resting on a rigid foundation was first developed by Housner [13]. He proposed a linear model to describe the rocking motion of slender blocks, highlighting, with the definition of "inverted pendulum", how the frequency parameter of the blocks depends on their size and on the gravitational acceleration but not on their mass. His pioneering work, moreover, provided a simple expression of the coefficient of restitution only depending on the slenderness; it represents an upper bound of the loss of energy due to the impact of the block on the ground. Housner defined the overturning conditions under horizontal actions schematized as single rectangular or half-sine impulse of acceleration; however, his analysis highlighted the difficulty to identify a stable relation between the geometric features of the block (size and slenderness) and the characteristics of the seismic input, so that the problem could only be treated through probabilistic approaches. This difficulty was also confirmed by the works of many other authors [14-17] who have examined the response of the block using both real or simulated accelerograms and harmonic loadings, highlighting the great sensitivity of the response to small variations in both system parameters and ground motion details. On the other hand, also other approaches ([18], [19]) based on response spectra have concluded that rocking block cannot be treated as an "equivalent" elastic SDOF because substantial differences are recognizable in its dynamic behavior.

Over the last years, increasing attention has been focused on the identification of the worst input scenario corresponding to the resonant response of the blocks and of single-degree-of-freedom (SDOF) inelastic structures [20-24]. In particular, the pioneering works by Casapulla et al. [20] and Casapulla [24] proposed a simplified representation of the seismic input as a sequence of instantaneous impulses of acceleration and identified the resonant condition with a time interval between these impulses coincident with the amplitude-dependent durations of the half-cycles of the motion. This approach allows describing the response of the block within the generic half-cycle as a natural motion. A powerful simplification of the equation of the motion was also proposed by the authors and a simply criterion of minimization of the error was validated through a comparison with the Housner model [25], [26].

More recently Kojima et al. [27] and Kojima and Takewaki [28] have proposed to schematize the impulsive component of a near-fault earthquake as a double impulse. Such a kind of input has been first used to identify the resonant condition of elastic-plastic systems and then extended by Nabeshima et al. [29] to obtain closed-form overturning limit for rigid blocks. This simplification has also been used to represent long duration earthquakes as a multiple impulse input [30]. Many other implications can be derived by simulating the near-field ground motions, which contain long-period directivity pulses [31, 32].

In this paper the analysis of rocking motion of large and slender rigid blocks is developed with reference to the intense phase of the seismic action described through an artificial accelerogram. In particular, this artificial accelerogram is described in Section 2 as resulting from the superposition of two sequences of instantaneous impulses: a main sequence, acting when the block impacts on the ground, defines the resonant condition; a secondary sequence of intermediate impulses, acting within the half-cycles, is then introduced in order to obtain a more realistic input condition. The closed-form equations governing the response of the block to the resonant sequence and a step-by-step procedure to obtain the response in the presence of intermediate impulses are presented in Section 3. Lastly, in Section 4 numerical results are presented, which take into account the effect of the amplitude of the intermediate impulses on the maximum response of the block and on the duration of the half-cycles, together with the influence of the restitution coefficient. Further developments of this study are contained in more extended works [33, 34].

2 ARTIFICIAL ACCELEROGRAMS AS SEQUENCES OF ISTANTANEOUS IMPULSES

The definition of the resonance condition for the rocking motion of rigid masonry blocks represents a basic reference in the analysis of their seismic response. Taking into account that the rocking motion is characterized by the oscillation of the blocks around the two vertex of the base with amplitude-dependent period, the maximization of the resonant effects has been obtained through an artificial accelerogram made up of sequences of instantaneous Dirac impulses; these impulses act at the beginning of each half-cycle of the rocking motion, right after the impact of the block on the ground. As a consequence the critical timing of impulses is not constant, but it increases with the duration of the half-cycle of the block oscillation, as schematically shown in Figure 1 [20]. The amplitude I of the single impulse of this accelerogram is defined through the integral of a half-wave of the ground horizontal acceleration assuming that the impulse is applied at the centroid of such a half-wave.

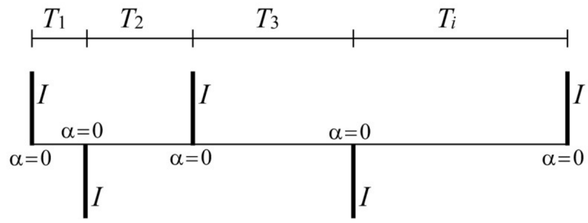

Figure 1: Limit artificial accelerogram as resonance sequence of instantaneous impulses.

This resonance sequence represents a theoretical input that allows investigating the rocking response to the worst input scenario, but it is quite unrealistic because, in particular, the critical timing of the impulses can be too long. Thereafter a secondary sequence of intermediate impulses acting during the half-cycle of motion of the block is introduced; this secondary sequence is also characterized by instantaneous impulses, all with the same amplitude $\underline{I_s}$, applied with alternate signs at equal time intervals $\underline{\Delta T}$ (the parameters and results referred to the secondary sequence are herein denoted by an underscore). The number of intermediate impulses between two subsequent impulses I of the limit accelerogram (main impulses), is an even number, so that their sum is zero (a typical property of all real accelerograms). Hence the secondary sequence is characterized by only two variable parameters, the amplitude and the frequency of the impulses, and it fulfills two specific requirements: to reduce the resonance effects of the limit accelerogram and to represent, with appropriate calibration of a few parameters, a large range of effects caused by the intense phases of recorded accelerograms. The corresponding scheme is shown in Figure 2.

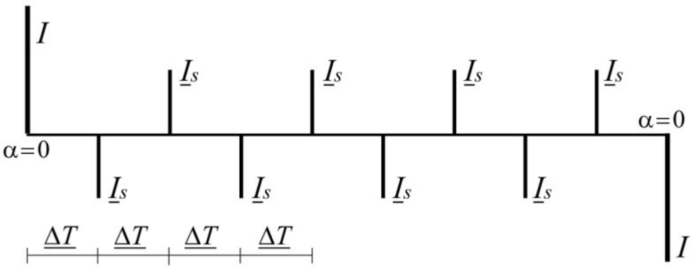

Figure 2: Secondary sequence of instantaneous intermediate impulses.

3 THE MODEL FOR THE ANALYSIS OF THE ROCKING MOTION OF THE BLOCKS

The hypothesis of instantaneous application of the impulses characterizing the seismic input described in the previous section allows treating the response of the block as a natural motion between two subsequent impulses. As well known, the natural motion of rigid free standing blocks, with slenderness $\lambda \geq 3$ ($\lambda = a/b$ in Figure 3), can be expressed by the linearized equation introduced by Housner [13]. Hence with the positive signs of forces and angles indicated in Figure 3, it is:

$$I_O\ddot{\alpha} + Mg(\alpha_c - \alpha) = 0 \qquad \Leftrightarrow \qquad \ddot{\alpha} + p^2(\alpha_c - \alpha) = 0 \tag{1}$$

in which M is the mass, $I_O = 4\,M(a^2+b^2)/3$ is the corresponding moment of inertia (with respect to O), $\alpha_c = \tan^{-1}(1/\lambda)$ is the maximum rotational angle of the block and $p = \sqrt{3g/(4R)}$ is the frequency parameter, being g the acceleration of gravity and R the half-diameter of the block.

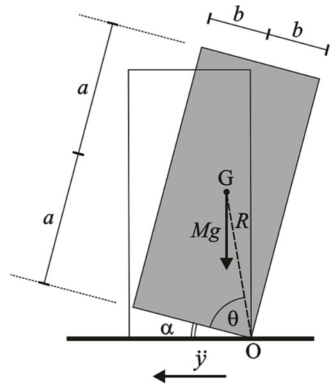

Figure 3: Rocking rigid block.

With the initial conditions $\alpha = \alpha_0$ and $\dot{\alpha} = \dot{\alpha}_0$, the solution of Eq. (1), in terms of rotational angle and velocity, is given by the following closed form expressions:

$$\alpha = \alpha_c + (A_1 - \alpha_c)\cosh pt + A_2 \sinh pt$$
$$\dot{\alpha} = (A_1 - \alpha_c) p \sinh pt + A_2 p \cosh pt \tag{2}$$

with the constants A_1 and A_2 depending on the initial conditions.

In the analysis it is assumed that the coefficient of friction is sufficiently large as to prevent sliding between the block and the supporting base, while the dissipation of the energy due to impact of the block on the ground is represented by the coefficient of restitution. This coefficient is assumed to be a variable of the problem to account also for other damping effects (e.g. local plastic deformations).

3.1 The response to the artificial resonance input

Each impulse I of the resonance sequence is applied immediately after the impact of the block on the ground ($\alpha = 0$) and causes an increment $\dot{\alpha}_1$ of the rotational velocity which is defined by the law of conservation of the angular momentum [20], [29]:

$$\dot{\alpha}_1 = \frac{M\, I\, a}{I_O} = \frac{\lambda \ddot{\alpha}_g\, I}{g} \tag{3}$$

where $\ddot{\alpha}_g$ is given by:

$$\ddot{\alpha}_g = \frac{3}{4}\frac{b}{a^2 + b^2}\, g \tag{4}$$

Let C denote the coefficient of restitution. The rotational velocity at the beginning of the generic half-cycle of the motion between two subsequent impacts is:

$$\dot{\alpha}_i = \dot{\alpha}_{i-1} C + \dot{\alpha}_1 = \dot{\alpha}_1 \left[\left(1 + \sum_{j=1}^{i-1} C^j \right) - C^{i-1} \right] \tag{5}$$

Assuming $\alpha(0) = 0$ and $\dot{\alpha}(0) = \dot{\alpha}_i$ as initial conditions for the half-cycle i, the constants in Eqs. (2) take the values $A_{1i} = 0$ and $A_{2i} = \dot{\alpha}_i / p$.

The maximum rotational angle, reached when $\dot{\alpha} = 0$, is:

$$\alpha_{i\max} = \alpha_c \left[1 - \cosh\left(\tanh^{-1} \frac{\dot{\alpha}_i}{\alpha_c p} \right) \right] + \frac{\dot{\alpha}_i}{p} \sinh\left(\tanh^{-1} \frac{\dot{\alpha}_i}{\alpha_c p} \right) \tag{6}$$

while the duration of the half-cycle i is:

$$\frac{T_i}{2} = \frac{2}{p} \tanh^{-1} \frac{\dot{\alpha}_i}{\alpha_c p} \tag{7}$$

Eq. (7) is similar to the formulation proposed by Housner [13] for the duration of the half-cycle, but it is expressed in terms of initial rotational velocity rather than in terms of initial rotational angle. Being $\tanh(x) < 1$, the validity of Eqs. (6) and (7) is restricted to the condition:

$$\frac{\dot{\alpha}_i}{\alpha_c p} = \frac{\dot{\alpha}_i}{\dot{\alpha}_c} < 1 \tag{8}$$

which also represents the safe region for $\dot{\alpha}_i$ to prevent overturning, as it can easily been verified by equating Eq. (6) to α_c. This limiting initial velocity, say $\dot{\alpha}_c = \alpha_c p$, also depends on the slenderness and the base dimension, consistently with the frequency parameter as showed in [25], [26].

By equating Eq. (5) to the critical velocity $\dot{\alpha}_c$, it is possible to define from Eq. (3) the critical value I_{ic} of the impulse causing overturning at the half-cycle i. It is:

$$I_{ic} = \frac{g\dot{\alpha}_c}{\lambda\ddot{\alpha}_g}\left[\left(1+\sum_{j=1}^{i-1}C^j\right)-C^{i-1}\right]^{-1} \tag{9}$$

It results that the impulse causing overturning at a fixed half-cycle i increases with decreasing slenderness and coefficient of restitution and with increasing size of the block. The increasing of I_{ic} implies of course that the block is less vulnerable to overturning.

It is worth highlighting that assuming $i = 2$ in Eq. (9), the value of the critical impulse I_{2c} is comparable with the velocity V_c of the critical double impulse defined by Nabeshima et al. [29] used to describe the impulsive component of the near-fault earthquakes.

At last, iterating Eq. (5) for $i \to\infty$, it is obtained that the rotational velocity does not increase indefinitely but converges to the limit value $\dot{\alpha}^*$ given by:

$$\dot{\alpha}^* = \lim_{i\to\infty}\dot{\alpha}_i = \frac{\dot{\alpha}_1}{1-C} \tag{10}$$

This case implies that, when overturning does not occur before, also the duration of the half-cycles tends to stabilize so that the motion of the block becomes of periodic type. An extensive parametric analysis of the influence of slenderness, size and coefficient of restitution of the block on the attainment of this stabilized phase was developed in [24].

3.2 The response to the secondary sequence of intermediate impulses

When a secondary sequence of intermediate impulses is taken into account, a step-by-step procedure is required to describe the motion of the block between two subsequent impacts. This motion, however, is still treated as a natural motion according to Eqs. (2), but the constants A_1 and A_2 have to be up dated at the application of each intermediate impulse $\underline{I}_s$. The increment of rotational velocity $\underline{\dot{\alpha}}_s$ caused by a single intermediate impulse is approximately evaluated as:

$$\underline{\dot{\alpha}}_s = \frac{\underline{I}_s}{I}\dot{\alpha}_1 \tag{11}$$

The procedure required to describe the rocking motion in the presence of intermediate impulses between two subsequent impacts is herein presented with reference to the first half-cycle, but it is also suitable for the generic half-cycle with assigned initial rotational velocity. This procedure implies the following steps:

1. Assign the main impulse I and compute the initial velocity $\dot{\alpha}_1$ by Eq. (3).
2. Compute the duration $T_1/2$ of the half-cycle by Eq. (7).
3. Select a trial value $\underline{\Delta T}$ of the time interval between two intermediate impulses ($\underline{\Delta T} < T_1/2$).
4. Compute step-by-step the rotational angle and velocity at each application of the intermediate impulses $\underline{I}_s$ by using Eqs. (2). Find approximated $\underline{T}_1 = \underline{n}\ \underline{\Delta T}$ at α close to zero ($\underline{n}$ is the number of $\underline{I}_s$ within the half-cycle).
5. Correct $\underline{\Delta T}$, and therefore $\underline{T}_1$, such that $\alpha(\underline{T}_1) = 0$ by strictly imposing the condition to have an even number $\underline{n}$ of intermediate impulses.

6. Compute step-by-step, with the corrected $\underline{\Delta T}$, the rotational angle and the velocity at each application of the intermediate impulses $\underline{I}_s$ by using Eqs. (2) and obtain the maximum angle of rotation $\underline{\alpha}_{1\max}$ and the rotational velocity at the end of the half-cycle $\dot{\underline{\alpha}}_{1r}$. Compute the initial velocity $\dot{\alpha}_{i=2}$ of the subsequent half-cycle by Eq. (5), using $\dot{\underline{\alpha}}_{i\text{-}1r}$ instead of $\dot{\underline{\alpha}}_{i\text{-}1}$.

4 PARAMETRIC ANALYSIS AND DISCUSSION OF THE RESULTS

The response of the block to the resonance input corrected with the secondary sequence of impulses has been investigated assuming that the so defined input represents the intense phase of an earthquake with duration limited to 20 s. Figure 4 shows the role of the main parameters characterizing the seismic input and of the coefficient of restitution on the maximum angle of rotation obtained within the limited time of 20 s; in fact, the $\underline{\alpha}_{\max}/\alpha_c$ ratio is plotted vs. different values of the intermediate impulses measured by the $\underline{I}_s / I$ ratio, for different values of the main impulses, expressed by the I / I_{1c} ratio, being I_{1c} the critical impulse for the first half-cycle (Eq. (9) with $i = 1$). Only values comprised between 0.3 and 0.7 are considered for $\underline{I}_s / I$ since values of $\underline{I}_s / I < 0.3$ are unrealistic, while large $\underline{I}_s / I$ ratios ($\underline{I}_s / I > 0.7$) imply less resonance effects, as will be shown. These non-dimensional parameters allow obtaining results independent of the geometric features of the blocks (block dimension and slenderness) and only dependent on the amplitude of the impulses and on the coefficient of restitution.

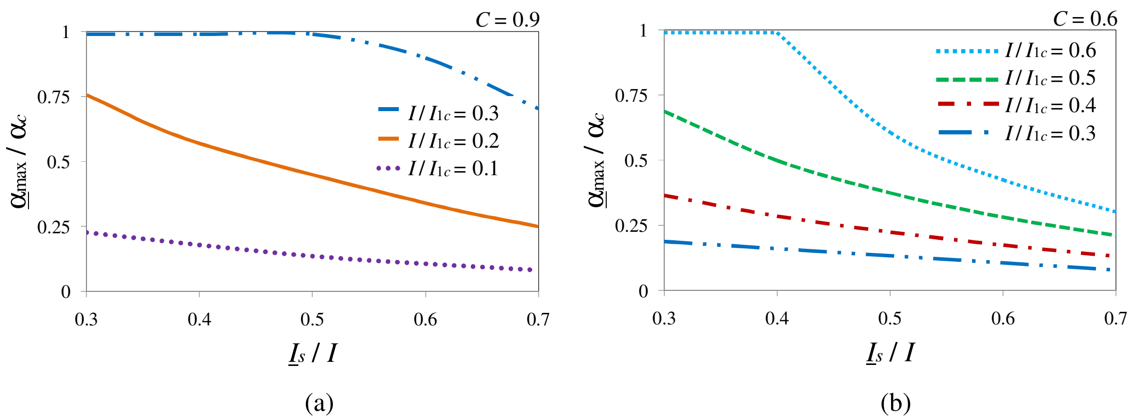

Figure 4: Values of $\underline{\alpha}_{\max}/\alpha_c$ related to a limited duration of the seismic input (20 s) vs. $\underline{I}_s / I$ ratio for different values of the I / I_{1c} ratio, with (a) $C = 0.9$ and (b) $C = 0.6$.

The curves in Figure 4 show that the secondary impulses $\underline{I}_s$ play an opposite role with respect to the impulses I of the limit accelerogram. In fact, for a fixed value of the I / I_{1c} ratio, the maximum angle of rotation is decreasing with increasing $\underline{I}_s / I$ ratio. The intermediate impulses have therefore a stabilizing effect, increasing with their amplitude. This trend can be explained by the consideration that large $\underline{I}_s / I$ ratios imply large variations of the rotational velocity with alternate sign at each application of the intermediate impulses, causing the angle of rotation to decrease. Conversely, if the $\underline{I}_s / I$ ratio is fixed, the increase in the amplitude of the impulses I implies the increase of $\underline{\alpha}_{\max}/\alpha_c$, as easily predictable.

The influence of the coefficient of restitution is evaluated by comparing Figs. 4(a) and 4(b), related to the results obtained for $C = 0.9$ and $C = 0.6$, respectively. Obviously larger values of C, with the other parameters kept constant, imply the increase of the destabilizing effects.

To investigate the influence of the geometric features of the blocks on the time evolution of their rocking response, two blocks with the same size ($2b = 1$ m) and different slenderness

($\lambda \approx 4$ when $R = 2$ m and $\lambda \approx 8$ when $R = 4$ m) are compared (Figure 5), taking into account the reference values of the restitution coefficient previously introduced ($C = 0.6$ and $C = 0.9$). The amplitude of the main impulses is assumed coincident with that of the critical impulse I_{2c} (Eq. (9) with $i = 2$) causing overturning at the second half-cycle if the secondary sequence is not taken into account ($\underline{I}_s / I = 0$). As already pointed out, the amplitude of this impulse is lower for the more slender block and also depends on the restitution coefficient. The reference to I_{2c} for the main impulses allows to compare the results related to $\underline{I}_s / I = 0$ with the results obtained by Nabeshima et al. [29] by considering the critical double impulses V_c. However, it must be remarked that in the present analysis the restitution coefficient C is a constant value independent of the slenderness of the blocks, while Nabeshima et al. [29] use the formulation proposed by Housner to define this parameter. Despite this, for $C = 0.9$ a very good agreement can be observed between the two formulations in terms both of the amplitudes of the main impulses and of the critical timings t_0 of application of the second impulse.

In Figure 5 the time-history responses of the two chosen blocks are reported in terms of the $\underline{\alpha}(t) / \alpha_c$ ratio, for different values of $\underline{I}_s / I$ and C.

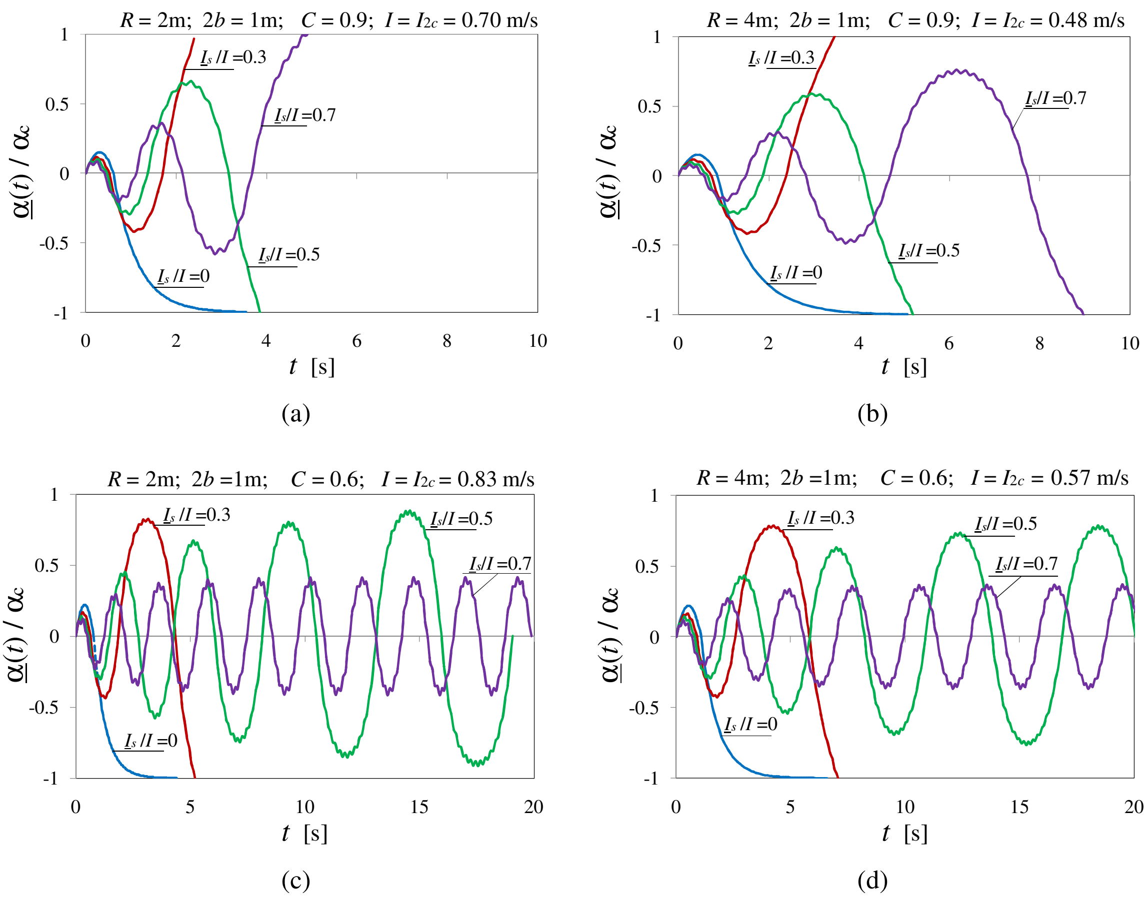

Figure 5: Time-history responses in terms of $\underline{\alpha}(t)/\alpha_c$ of two blocks with $2b = 1$ m and $R = 2$ m ((a), (c)) and $R = 4$ m ((b), (d)), related to the critical impulse I_{2c}, for different values of $\underline{I}_s / I$ and C.

First of all, these curves show that for each block the action of the intermediate impulses not only implies the reduction of the maximum rotation angle at each half-cycle, but also the reduction of the duration of the same half-cycles. These effects are increasing with increasing $\underline{I}_s / I$ ratios. In fact, when $\underline{I}_s / I \neq 0$, both blocks do not overturn at the second half-cycle but perform a number of half-cycles increasing with $\underline{I}_s / I$. For a fixed value of this ratio and of the restitution coefficient, the influence of the different slenderness of the two blocks - only due to the different values of R, being the size $2b$ constant - is manly expressed in the reduction of the duration of the half-cycles, so that the more slender block (R = 4 m) achieves the overturning in a longer time than the other (R = 2 m), although performing the same number of half-cycles (Figs. 5(a) and 5(b)). The case of $\underline{I}_s / I = 0.7$ implies a slight increment also of the number of half-cycles for the more slender block. The higher stability of the more slender block is justified in this case by the lower amplitude of the main impulse.

Lastly, the effect of the lower value of the restitution coefficient on the obtained results, keeping constant the other parameters, is confirmed in terms of reduction of the maximum angle of rotation and of the duration of the half-cycles, while their number increases in the limit duration of 20 s of the input. Moreover, when $C = 0.6$, with increasing values of $\underline{I}_s / I$, both the blocks tend to reach a stabilized phase characterized by a periodic motion with constant values of the maximum rotational angle at each half-cycle and of the duration of these half-cycles.

5 CONCLUSIONS

The great sensitivity of the rocking response of rigid blocks to small variations of the seismic action makes very difficult to define a stable relation to their geometric features and the parameters characterizing the seismic input. Starting from this consideration, widely confirmed by the scientific literature on this subject, the approach proposed in this paper consists in the definition of simplified artificial accelerograms characterized by few parameters, both capable of representing the most unfavorable effects of the intense phase of an earthquake and of covering the widest range of real accelerograms.

First, the resonant conditions for the rocking motion were investigated by means of a main sequence of instantaneous impulses applied just after the impact of the block on the ground; then a secondary sequence of intermediate impulses acting within the half-cycle of the block motion was introduced. The intent was to obtain a parametric model of accelerogram that can reproduce the same effects of any registered accelerogram, trough a proper calibration of the characteristic parameters, i.e the amplitudes of the impulses of both the main and the secondary sequence and the time interval of the secondary impulses.

The critical response of the block to the proposed accelerogram, represented by the achievement of the overturning, has resulted to be mainly affected by the following issues: the size and slenderness of the rigid block; the amplitudes of the main and of the intermediate impulses, the restitution coefficient. The analysis enables, in particular, to distinguish the actions which cause overturning from those that cause the stabilization of the motion in relation with the influencing parameters. It was also shown that the increasing amplitude of the intermediate impulses implies not only the reduction of the maximum response of the block, but also the duration of the half-cycles of the motion. The opposite trend was reported for increasing values of the coefficient of restitution; with the other parameters kept constant, in fact, the maximum response of the block and the duration of the half-cycles are increasing with this coefficient.

Clearly, the specification of the parameters that characterize the artificial accelerogram should be depending on the specific characteristics of the sites. This aspect could be the further developed in order to apply the proposed procedure to real accelerograms. On the other hand, the synthesis of the various aspects can allow translating clear specific indications in final sufficiently reliable evaluations.

ACKNOWLEDGEMENTS

The authors acknowledge the sponsorship of the Italian Civil Protection, through the RELUIS Project - Line: Masonry Structures (2017).

REFERENCES

[1] L. Giresini, Energy-based method for identifying vulnerable macro-elements in historic masonry churches. *Bulletin of Earthquake Engineering*, **44**(13), 919-942, 2015.

[2] C. Casapulla, A. Maione, L.U. Argiento, Seismic analysis of an existing masonry building according to the multi-level approach of the Italian Guidelines on Cultural Heritage. *Ingegneria Sismica*, **1**, 2017, 1-21.

[3] C. Casapulla, Dry rigid block masonry: Safe solutions in presence of Coulomb friction. *Advances in Architecture Series*, **7**, 251-261, 2001.

[4] C. Casapulla, L. Cascini, F. Portioli, R. Landolfo, 3D macro and micro-block models for limit analysis of out-of-plane loaded masonry walls with non-associative Coulomb friction. *Meccanica*, **49**(7), 1653-1678, 2014.

[5] C. Casapulla, F. Portioli, Experimental and analytical investigation on the frictional contact behavior of 3D masonry block assemblages. *Construction and Building Materials*, **78**, 126-143, 2015.

[6] C, Casapulla, A. Maione, Formulating the torsion strength of dry-stacked stone blocks by comparing convex and concave contact formulations and experimental results. *Indian Journal of Science and Technology*, 9(46), 107346, 2016.

[7] C. Casapulla, L.U. Argiento, The comparative role of friction in local out-of-plane mechanisms of masonry buildings. Pushover analysis and experimental investigation. *Engineering Structures,* **126**, 158-173, 2016.

[8] C. Casapulla, L.U. Argiento, Non-linear kinematic analysis of masonry walls out-of-plane loaded. the comparative role of friction between interlocked walls. *6th International Conference on Computational Methods in Structural Dynamics and Earthquake Engineering*, Rhodes Island, Greece, June 15-17, 2017.

[9] C. Casapulla, L.U. Argiento, C. Ceraldi, Experimental validation of in-plane frictional resistances in dry block masonry walls. *6th International Conference on Computational Methods in Structural Dynamics and Earthquake Engineering*, Rhodes Island, Greece, June 15-17, 2017.

[10] L. Giresini, M. Sassu, Horizontally restrained rocking blocks: evaluation of the role of boundary conditions with static and dynamic approaches. *Bulletin of Earthquake Engineering*, **15**(1), 385-410, 2016.

[11] L. Giresini, M. Fragiacomo, M. Sassu, Rocking analysis of masonry walls interacting with roofs. *Engineering Structures*, **116**, 107-120, 2016.

[12] N. Makris, M.F. Vassiliou, Dynamics of the rocking frame with vertical restrainers. *Journal of Structural Engineering* (ASCE), **141**(10), 1-13,2015.

[13] G.W. Housner, The behaviour of inverted pendulum structures during earthquakes. *Bulletin of the Seismological Society of America,* **53**(2), 403-417, 1963.

[14] C.K. Yim, A.K. Chopra, J. Penzien, Rocking response of rigid blocks to earthquakes. *Earthquake Engineering and Structural Dynamics*, **8**(6), 565-587, 1980.

[15] M. Aslam, W.G. Godden, D.T. Scalise, Earthquake rocking response of rigid bodies. *Journal of Engineering Mechanics ASCE*, **106**(2), 377-392, 1980.

[16] P.D. Spanos, A.S. Koh, Rocking of rigid blocks due to harmonic shaking. *Journal of Engineering Mechanics ASCE*, **110**(11), 1627-1642, 1984.

[17] S.J. Hogan, On the dynamics of rigid-block motion under harmonic forcing. *Proceedings of Royal Society A,* **425**(1869), 441–476, 1989.

[18] N. Makris, D. Konstantinidis, The rocking spectrum and the limitations of practical design methodologies. *Earthquake Engineering and Structural Dynamics*, **32**(2), 265-289, 2003.

[19] S. Lagomarsino, Seismic assessment of rocking masonry structures. *Bulletin of Earthquake Engineering*, **13**(1), 97-128, 2015.

[20] C. Casapulla, P. Jossa, A. Maione, Rocking motion of a masonry rigid block under seismic actions: a new strategy based on the progressive correction of the resonance response. *Ingegneria Sismica*, **27**(4), 35-48, 2010.

[21] A. Moustafa, K. Ueno, I. Takewaki, Critical earthquake loads for SDOF inelastic structures considering evolution of seismic waves. *Earthquake and Structures*, **1**(2), 147-162, 2010.

[22] I. Takewaki, *Critical Excitation Methods in Earthquake Engineering, 2nd Edition*. Elsevier, 2013.

[23] I. Takewaki, A. Moustafa, K. Fujita, *Improving the Earthquake Resilience of Buildings: The Worst Case Approach*. Springer-Verlag, London, 2013.

[24] C. Casapulla, On the resonance conditions of rigid rocking blocks. *International Journal of Engineering and Technology*, **7**(2), 760-771, 2015.

[25] C. Casapulla, A. Maione, Free damped vibrations of rocking rigid blocks as uniformly accelerated motions. *International Journal of Structural Stability and Dynamics* [online], September 2016, http://dx.doi.org/10.1142/S0219455417500584.

[26] C. Casapulla, A. Maione, A simplified equation of motion for free rocking rigid blocks. *Insights and Innovations in Structural Engineering, Mechanics and Computation*, 120-126, Cape Town, South Africa, September 2016.

[27] K. Kojima, K. Fujita, I. Takewaki, Critical double impulse input and bound of earthquake input energy to building structure. *Frontiers in Built Environment*, **1**(5), 1-8, 2015.

[28] K. Kojima, I. Takewaki, Critical earthquake response of elastic-plastic structures under near-fault ground motions (part 1: fling-step input). *Frontiers in Built Environment*, **1**(12), 1-11, 2015.

[29] K. Nabeshima, R. Taniguchi, K. Kojima, I. Takewaki, Closed-form overturning limit of rigid block under critical near-fault ground motions. *Frontiers in Built Environment*, **2**(9), 1-11, 2016.

[30] K. Kojima, I. Takewaki, Critical input and response of elastic-plastic structures under long-duration earthquake ground motions. *Frontiers in Built Environment*, **1**(15), 1-13, 2015.

[31] I.N. Psycharis, M. Fragiadakis, I. Stefanou, Seismic reliability assessment of classical columns subjected to near-fault ground motions. *Earthquake Engineering and Structural Dynamics*, **42**(14), 2061-2079.

[32] E.G. Dimitrakopoulos, T.S. Paraskeva, Seismic reliability assessment of rocking behaviour under near-fault excitations. *5th ECCOMAS Thematic Conference on Computational Methods in Structural Dynamics and Earthquake Engineering*, Crete Island, Greece, May 25-27, 2015.

[33] C. Casapulla, A. Maione, Critical response of free-standing rocking blocks to the intense phase of an earthquake. *International Review of Civil Engineering*, **8**(1), 1-10, 2017.

[34] C. Casapulla, P. Jossa, A. Maione, A simplified procedure for the seismic safety of large and slender rigid masonry blocks. *International Journal of Earthquake and Impact Engineering*, **1**(4), 333-359, 2016.